[8] W. F. Richards, J.-D. Ou, and S. A. Long, "A theoretical and experimental investigation of annular, annular sector, and circular sector microstrip antennas," *IEEE Trans. Antennas Propag.*, vol. 32, no. 8, pp. 864–867, Aug. 1984.
[9] A. Das, S. P. Mathur, and S. K. Das, "Radiation characteristics of higher-order modes in microstrip ring antenna," *IEE Proc. H Microw., Opt. Antennas*, vol. 131, no. 2, pp. 102–106, Apr. 1984.
[10] I. Wolff and V. K. Tripathi, "The microstrip open-ring resonator," *IEEE Trans. Microw. Theory Techn.*, vol. 32, no. 1, pp. 102–107, Jan. 1984.
[11] W. C. Chew, "A broad-band annular-ring microstrip antenna," *IEEE Trans. Antennas Propag.*, vol. 30, no. 5, pp. 918–922, Sep. 1982.
[12] J. Zhang, Y. Li, Z. Liang, S. Zheng, and Y. Long, "Design of a multifrequency one-quarter-rings microstrip antenna," *IEEE Antennas Wireless Propag. Lett.*, vol. 14, pp. 209–212, 2015.
[13] M. A. Sultan, "The mode features of an ideal-gap open-ring microstrip antenna," *IEEE Trans. Antennas Propag.*, vol. 37, no. 2, pp. 137–142, Feb. 1989.
[14] G. Kumar and K. C. Gupta, "Nonradiating edges and four edges gap-coupled multiple resonator broad-band microstrip antennas," *IEEE Trans. Antennas Propag.*, vol. 33, no. 2, pp. 173–178, Feb. 1985.
[15] G. Kumar and K. C. Gupta, "Broad-band microstrip antennas using additional resonators gap-coupled to the radiating edges," *IEEE Trans. Antennas Propag.*, vol. 32, no. 12, pp. 1375–1379, Dec. 1984.
[16] J. Liu, S. Zheng, Y. Li, and Y. Long, "Broadband monopolar microstrip patch antenna with shorting vias and coupled ring," *IEEE Antennas Wireless Propag. Lett.*, vol. 13, pp. 39–42, 2014.
[17] R. P. Owens, "Curvature effect in microstrip ring resonators," *Electron. Lett.*, vol. 12, no. 14, pp. 356–357, Jul. 1976.
[18] M. A. Sultan and V. K. Tripathi, "The mode features of an annular sector microstrip antenna," *IEEE Trans. Antennas Propag.*, vol. 38, no. 2, pp. 265–269, Feb. 1990.
[19] J. A. B. Faria, "A novel approach to ring resonator theory involving even and odd mode analysis," *IEEE Trans. Microw. Theory Techn.*, vol. 57, no. 4, pp. 856–862, Apr. 2009.

Human Activity Classification Based on Dynamic Time Warping of an On-Body Creeping Wave Signal

Yang Li, Dong Xue, Erik Forrister, George Lee, Brian Garner, and Youngwook Kim

***Abstract*— The characteristics of a nonline-of-sight on-body creeping wave are utilized to classify human motion activities. Creeping wave propagation around the torso of a nonmoving human is reviewed. Its associated complex transmission data are measured for six different motion activities on both male and female subjects. A dynamic time warping algorithm is applied on the signal magnitude and phase data for pattern recognition. The study is extended to different on-body channels and frequencies for comparisons.**

***Index Terms*— Creeping wave, dynamic time warping (DTW) algorithm, human activity classification, on-body electromagnetic (EM) wave propagation.**

I. Introduction

Electromagnetic (EM) wave propagation over the human body surface has attracted great interest in recent years due to the promising future of wireless body area network (WBAN) technology [1]. A typical WBAN consists of several wearable body sensor nodes which continuously record and send physiological data to a body control unit (e.g., smart phone) for applications including remote health monitoring, battlefield communication, personal entertainment, and human space flight [2]. Understanding how EM waves propagate along or around the human body is critical for designing a reliable and efficient WBAN. Driven by this need, researchers have conducted extensive studies over the past decade, and have discovered that both space wave and surface wave effects can occur for line-of-sight (LOS), along-body propagation, whereas creeping wave effects dominate for non-LOS (NLOS), around-body propagation [3].

More recently, researchers have sought to exploit the on-body wireless propagation characteristics for human activity recognition [4]–[6]. Guraliuc *et al.* [4] used wearable wireless transceivers to classify limb movements. Munoz *et al.* [5] applied frequency analysis to identify four different activities, and proposed extracting more biomechanical information from dynamical WBAN channels. Wang and Zhou [6] reviewed activity recognition techniques based on body area radios such as Zigbee, Wifi, and RFID. Compared to traditional activity recognition methods, which rely on specialized physical sensors (motion camera, accelerometer, gyroscope, etc.), the on-body propagation methods are low-cost, power-efficient, and can provide high classification accuracy. However, most studies to date have utilized only signal magnitudes (RSS) of LOS space wave propagation at 2.45 GHz. In this communication, we investigate using both the magnitude and phase of NLOS creeping waves for motion pattern recognition. We further explore the optimum of different

Manuscript received December 30, 2015; revised May 13, 2016; accepted July 26, 2016. Date of publication August 4, 2016; date of current version October 27, 2016. This work was supported by the NSF under Grant ECCS-1609371.

Y. Li, D. Xue, E. Forrister, G. Lee, and B. Garner are with the School of Engineering and Computer Science, Baylor University, Waco, TX 76798 USA (e-mail: yang_li1@baylor.edu).

Y. Kim is with the Department of Electrical and Computer Engineering, Lyles College of Engineering, California State University, Fresno, CA 93740-8030 USA (e-mail: youngkim@csufresno.edu).

Color versions of one or more of the figures in this communication are available online at http://ieeexplore.ieee.org.

Digital Object Identifier 10.1109/TAP.2016.2598199

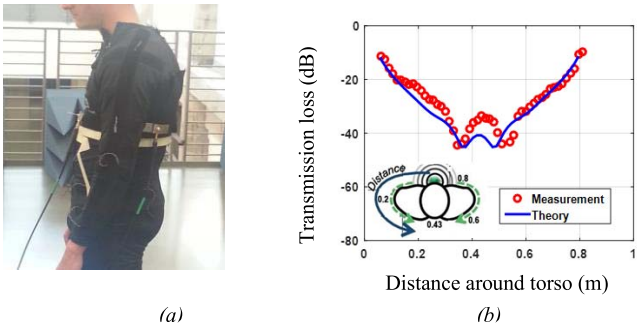

Fig. 1. (a) On-body creeping wave measurement setup. (b) Measured transmission data at 915 MHz along with theoretical values from [9].

antenna placements (channels) and antenna operating frequencies for human activity classification.

To address these scientific questions, we measure creeping wave transmission on both male and female subjects for six different activities at 433 MHz, 915 MHz, and 2.45 GHz WBAN frequency bands. We then apply, and assess the computational efficiency of, a dynamic time warping (DTW) algorithm to classify activities based on magnitude and phase of the transmission data. We extend the study to include three on-body propagation channels commonly used for WBAN applications, and analyze the results to help identify the best channel and its associated best operating frequency.

This communication is organized as follows. Section II reviews the on-body creeping wave mechanism. Section III describes the six human motion activities, and presents measurement setup and results. The classification algorithm is introduced and implemented in Section IV. Section V reports the test outcomes and compares the recognition results among different on-body channels and different operating frequencies. Section VI provides discussion and conclusions.

II. Review of On-Body Creeping Wave Propagation

On-body creeping wave propagation was first proposed in [7] based on finite difference time domain simulations of a numerical human phantom model. It was observed that the EM wave decays exponentially as it travels around the human torso, a result also supported by *in situ* measurement data [8]. Alves *et al*. [9] formally derived an analytical path loss model from the diffraction theory that describes creeping wave attenuation along a circular path around a lossy dielectric cylinder. Their theory predictions show good agreement with both simulations and measurements.

To illustrate on-body creeping wave propagation for the purpose of this communication, complex transmission data S_{21} are collected around the torso of one human subject at the 915 MHz industrial, scientific and medical (ISM) band. Fig. 1(a) shows the measurement setup: the transmitting antenna is placed at the front chest, and the receiving antenna is moved horizontally around the torso at the chest level with a step size of 3 cm. The human subject abducts both arms to the horizontal plane during the measurement to avoid interference of the creeping wave propagation path. Both transmitting and receiving antennas are constructed as quarter wavelength monopoles on a finite size ground plane ('bridge' monopole) and pointed normal to the body surface. A vector network analyzer (Agilent N5230C) is used to record measurements in the indoor, open hallway environment. Both transmitting and receiving antennas are connected to the vector network analyzer (VNA) by 3-m-long coaxial cables (Workhorse Plus-524).

Fig. 1(b) shows the normalized transmission data against the distance wrapping around the torso. Evidence of both clockwise and counter-clockwise creeping waves can be clearly observed, as well as their mutual interference at the back of the torso ($d = 0.43$ m). The creeping wave theory from [9] is also shown in the plot, and it shows good agreement with our measurement data.

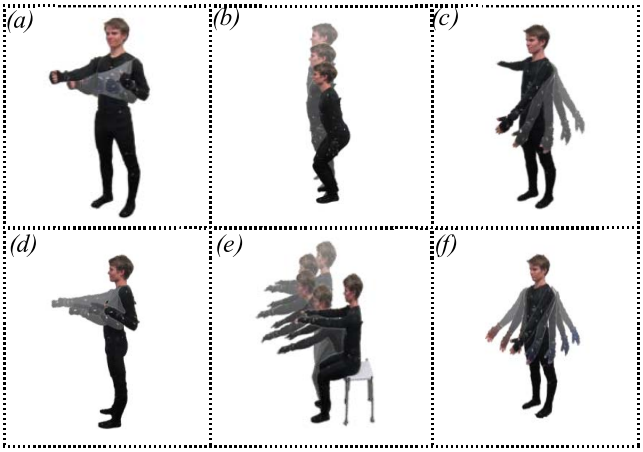

Fig. 2. Six human activities. (a) Boxing. (b) Hopping. (c) Left arm swing. (d) Rowing. (e) Sitting. (f) Both arms swing.

III. Dynamic Creeping Wave Measurements

Dynamic creeping wave propagation is measured using two antennas fixed, respectively, at the front and back torso of our participants. Three pairs of quarter-wave monopole antennas, centered at 433 MHz, 915 MHz, and 2.45 GHz, respectively, are used for different trials to cover WBAN frequency bands. As the human subjects are performing various activities, complex transmission data S_{21} are recorded using the VNA under continuous time mode with a sampling rate of 120 Hz.

Our dynamic measurements involve six different activities: 1) boxing; 2) hopping; 3) left arm swinging; 4) rowing; 5) sitting; and 6) both arms swinging, as illustrated in Fig. 2. The participants perform each activity continuously for 40 s, and for each of three repeated trials. Two participants are included in the experiments: 1) a 23 years male (171 cm height, 62 kg weight) and 2) a 25 years female (164 cm height, 50 kg weight).

Fig. 3 shows representative examples of the measured S_{21} parameters versus time for the six different activities at 915 MHz for male (solid blue line) and female (dashed red line) participants. The amplitude and unwrapped phase of the signals are normalized to 1° and 180° for pattern recognition. It can be clearly observed that both magnitude and phase data exhibit unique periodic features depending on the activity, which implies the creeping wave channel can potentially be used to classify dynamic human movements.

Similar observations can be made from the S_{21} measurements at 433 MHz and 2.45 GHz, as shown in Figs. 4 and 5, respectively, for two representative activities (boxing and both arms swinging). In both plots, the magnitude and phase are not normalized to facilitate comparison between different frequencies. It is seen that the signal magnitude decreases with the increase of frequency since the path loss is much larger for creeping waves at higher frequencies. The pattern at 2.45 GHz is difficult to recognize due to the low signal to noise ratio.

IV. Human Activity Classification With Dynamic Time Warping Technique

We apply a DTW algorithm to classify the human motion activities of our measured, time-varying transmission data. DTW facilitates

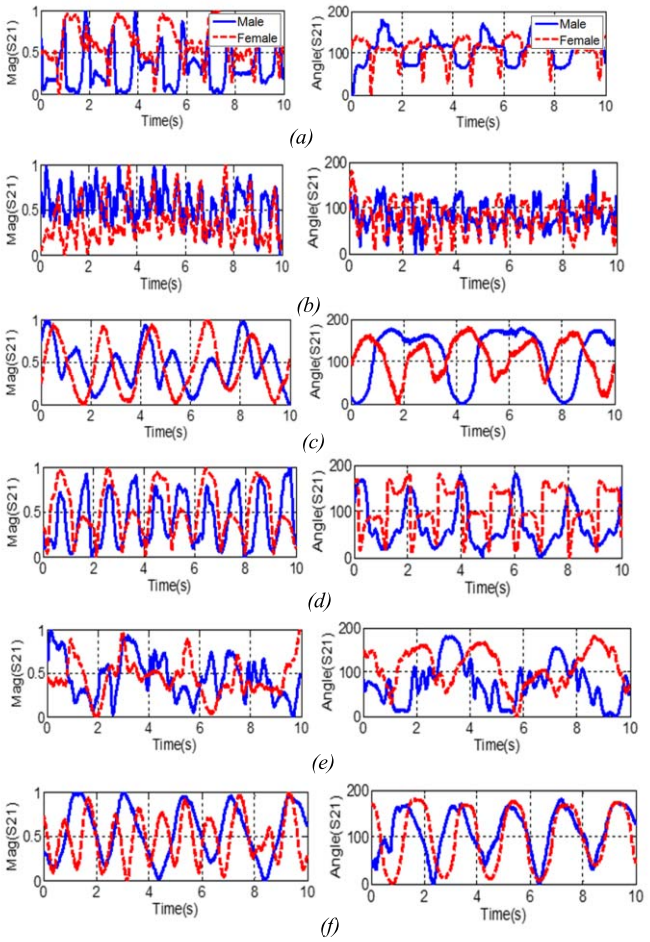

Fig. 3. Examples of the S_{21} parameters from chest to back antennas measured at 915 MHz for six human activities. (a) Boxing. (b) Hopping. (c) Left arm swing. (d) Rowing. (e) Sitting. (f) Both arms swing.

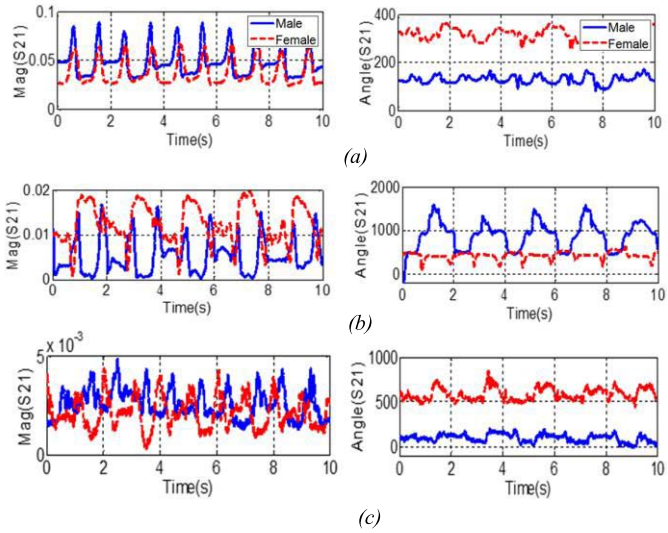

Fig. 4. Measured S_{21} parameters from chest to back antennas for the boxing activity at (a) 433 MHz, (b) 915 MHz, and (c) 2.45 GHz.

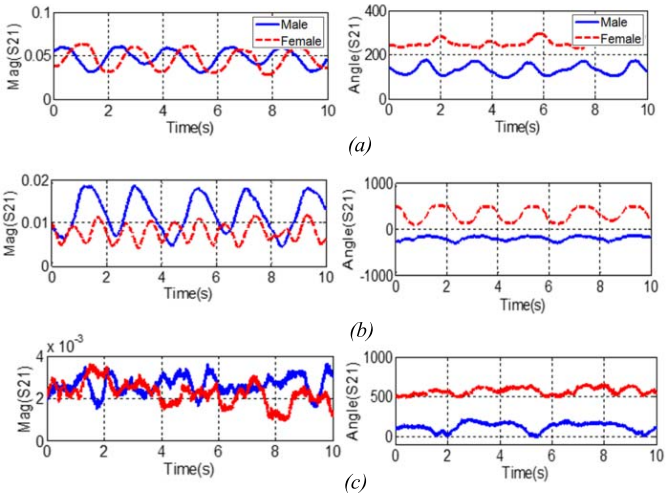

Fig. 5. Measured S_{21} parameters from chest to back antennas for both arms swinging at (a) 433 MHz, (b) 915 MHz, and (c) 2.45 GHz.

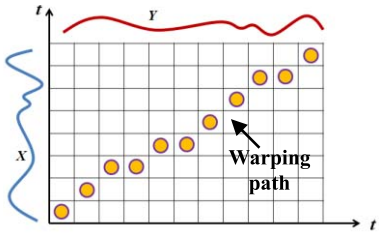

Fig. 6. Local cost matrix and a warping path between data sequences X and Y versus time t.

assessment of the similarity of two temporal signals when one has linear or nonlinear variations in time with respect to the other [10]. DTW compensates for such time variations, which may include delay offset, acceleration, and deceleration, by optimally warping the two signals in time so that corresponding features of the signals align properly. Once aligned, the signal similarities can be assessed. DTW has been applied in diverse fields including automatic speech recognition, video and graphic signal analysis, protein sequence alignment, partial shape matching, and micro-Doppler signature recognition [11]–[13]. We apply DTW in this study because the considered human motions are periodic, but can be executed at different or inconsistent rates from trial to trial.

The DTW algorithm works by creating a local cost matrix where each cell of the matrix represents the pair wise distance between samples of two data sequences, X and Y, as shown in Fig. 6. The matrix diagonal corresponds to the data remaining unwarped from the lower left cell (first sample of both sequences) to the upper right cell (last sample of both sequences). Off-diagonal cells represent data elements of one or both data sequences being shifted, or warped, in time. The DTW algorithm computes the optimal warping for each sequence by tracing a path from first to last sample such that a total cost function is minimized. The cost function is the sum of the local distance values of all cells traversed over the path. When the best path to cell i, j is defined as cell(i, j), then the next best next cell in the path can be found as

$$\begin{aligned}&\text{cell}(i+1, j+1)\\&= \text{local\_distance}(i+1, j+1) + \text{MIN}(\text{cell}(i, j+1), \text{cell}(i+1, j)).\end{aligned} \tag{1}$$

In our implementation of DTW, the data sequences (X or Y) come from our experimental trials. Each of these trials results in S_{21} magnitude and phase data versus time over multiple activity

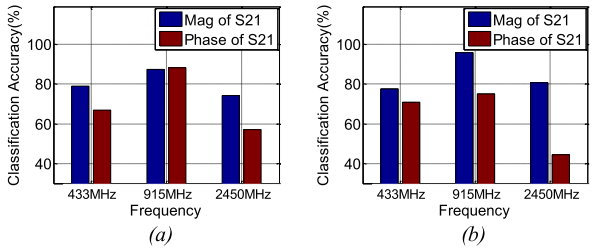

Fig. 7. Classification accuracy using magnitude and phase of S_{21} for (a) male subject and (b) female subject.

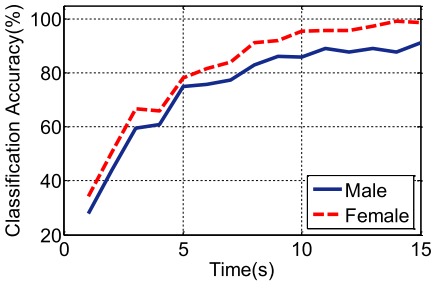

Fig. 8. Motion activity classification accuracy versus time window size.

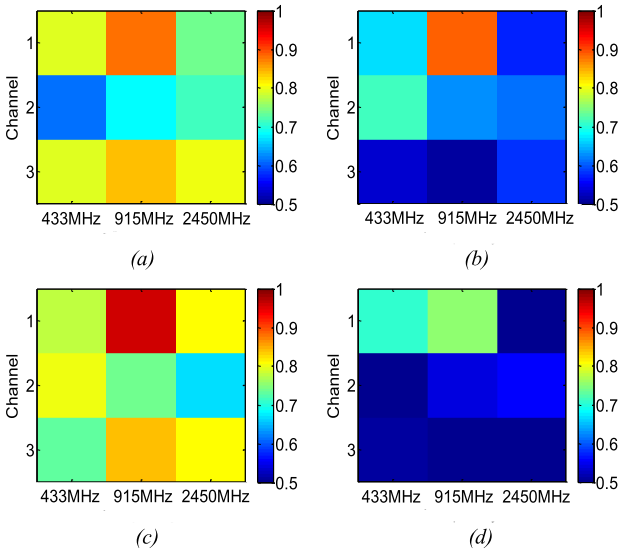

Fig. 9. Classification accuracy depending on different channels and frequencies. Male subject using (a) magnitude of S_{21} and (b) phase of S_{21}. Female subject using (c) magnitude of S_{21} and (d) phase of S_{21}.

cycles. As an example, X could be magnitude versus time for one trial of male subject 1, measured at 433 MHz, and performing the sitting activity. Then, Y could be magnitude versus time for another trial with the same frequency and subject performing the rowing activity. DTW permits us to quantify the similarity between any two experimental trials based on either the magnitude or phase data. Data from both trials are warped in time until they agree as closely as possible with each other. The resulting, post-warped accumulated distance (cost function) between the two trials represents their DTW similarity, with lowest distance value indicating greatest similarity.

To apply the DTW algorithm for activity classification we first select reference data to represent each of the six activities. We randomly select 10 s of magnitude and phase data from each of five trials of a known activity. We use five trials in order to include some level of variation in the reference data, and thus to reduce the risk of bias. To classify test data of an unknown activity, we compute an overall activity similarity between the test data and the reference data for each activity. The activity for which the activity similarity is best (i.e., least summed distance) is taken as the activity classification. We test this classification method for 40 sample data sets (10 s each) for each of the six activities (240 sample data sets total).

It should be pointed out that we use S_{21} data from the same subject for both reference and test purposes. This approach can be justified since the goal of this study is to apply a single user's on-body creeping wave channel to classify his/her own motion pattern. The creeping wave propagation can be different among different subjects due to body size, tissue properties, motion characteristics, etc., resulting in unique S_{21} signatures for each subject. The classification accuracy may decrease if we cross validate with multiple subjects.

V. Results and Discussion

Fig. 7(a) and (b) shows the DTW classification results over all activities based on the magnitude and phase of dynamic creeping wave signals for male and female subjects, respectively. The horizontal axis represents trials using three frequencies at 433, 915, and 2450 MHz, respectively, and the vertical axis reflects the classification accuracies. It is observed that the creeping wave data at 915 MHz generally provides the best classification results for both male and female subjects. This result is likely because the signal variation at 433 MHz, with its relatively large wavelength, is smaller than at the other frequencies, and because the information in the 2.45 GHz signal may be contaminated by low signal-to-noise ratio. The accuracy at 915 MHz for the male subject is 87.5% based on S_{21} magnitude and 88.3% based on S_{21} phase; the corresponding results for the female subject are 95.8% and 75.0%.

Our classification results are comparable to previous studies based on the LOS space wave. For example, Guraliuc *et al.* [4] report classification accuracies of 70% and 85% for two subjects using a two-feature study, and 90% and 100% using a five-feature study. Wang and Zhou [6] report classification accuracies of 86.3%, 92.5%, and 84.2% for three subjects, and propose grading experimental recognition performance as low (<60%), middle (<80% and >60%), or high (>80%). According to this scale, our results grade as high performance, suggesting that classification based on the creeping wave may be an effective approach.

To further explore this classification approach, we examine the impact of effective time window size on the classification accuracy. The time window should be large enough to capture at least one period of the human motion, which in our data extends from 2 to 4 s. A larger time window is preferable to improve the classification accuracy, but also increases the DTW computational cost. Fig. 8 shows the classification accuracy using the creeping wave at 915 MHz for different window sizes. The plots show that classification accuracy saturates at time windows larger than approximately 10 s.

Finally, we extend our study to compare classification results of the chest to back creeping wave channel (Ch.1) to two other commonly used on-body channels: the chest to the left wrist channel (Ch.2) and the left wrist to the right wrist channel (Ch.3). For these two additional channels we again measure the same human subjects performing the same six activities at the same three frequencies, and we repeat the DTW algorithm to post process the data. Fig. 9(a) and (b) shows classification results for the male subject based on S_{21} magnitude and phase. Fig. 9(c) and (d) shows the corresponding results for the female subject. Interestingly, it can be observed that the chest to back channel at 915 MHz offers the highest classification accuracy.

VI. Conclusion

We found that analysis of on-body creeping wave signals can be effective for classifying six human movement activities. We further

found that, among the three frequencies 433, 915, and 2400 MHz, the 915 MHz frequency provided the highest classification accuracy. Both magnitude and phase of the creeping wave transmission data provide enough unique signatures for good classification accuracy. For the activities studied, a 10-s time window size for the DTW classification algorithm offered the best tradeoff between classification accuracy and computational efficiency. Finally the chest-to-back creeping wave channel exceeded other on-body channels for providing the best classification accuracy.

Future work can improve upon this study by including more subjects to validate the effectiveness of the presented approach. Future work can also improve upon this study by including more operating environments, such as an indoor office or hospital room, to further assess the applicability of the proposed method. The sensitivity of sensor position and orientation to the classification accuracy can also be investigated. In addition, this research can be extended to explore more complex activities that include lower limb movements, where the leg movement may also alter characteristics of the creeping wave. Finally, more advanced signal processing algorithms can be incorporated to extract more physiological information from the dynamic channels, which could improve the classification performance.

REFERENCES

[1] P. S. Hall *et al.*, "Antennas and propagation for on-body communication systems," *IEEE Antennas Propag. Mag.*, vol. 49, no. 3, pp. 41–58, Jun. 2007.

[2] H. Cao, V. Leung, C. Chow, and H. Chan, "Enabling technologies for wireless body area networks: A survey and outlook," *IEEE Commun. Mag.*, vol. 47, no. 12, pp. 84–93, Dec. 2009.

[3] D. B. Smith, D. Miniutti, T. A. Lamahewa, and L. W. Hanlen, "Propagation models for body-area networks: A survey and new outlook," *IEEE Antennas Propag. Mag.*, vol. 55, no. 5, pp. 97–117, Oct. 2013.

[4] A. R. Guraliuc, P. Barsocchi, F. Potortì, and P. Nepa, "Limb movements classification using wearable wireless transceivers," *IEEE Trans. Inf. Technol. Biomed.*, vol. 15, no. 3, pp. 474–480, May 2011.

[5] M. O. Munoz, R. Foster, and Y. Hao, "Exploring physiological parameters in dynamic WBAN channels," *IEEE Trans. Antennas Propag.*, vol. 62, no. 10, pp. 5268–5281, Oct. 2014.

[6] S. Wang and G. Zhou, "A review on radio based activity recognition," *Digit. Commun. Netw.*, vol. 1, no. 1, pp. 20–29, Feb. 2015.

[7] J. Ryckaert, P. De Doncker, R. Meys, A. de Le Hoye, and S. Donnay, "Channel model for wireless communication around human body," *Electron. Lett.*, vol. 40, no. 9, pp. 543–544, Apr. 2004.

[8] P. S. Hall and Y. Hao, Eds., *Antennas and Propagation for Body-Centric Wireless Communications*. Boston, MA, USA: Artech House, 2006.

[9] T. Alves, B. Poussot, and J.-M. Laheurte, "Analytical propagation modeling of BAN channels based on the creeping-wave theory," *IEEE Trans. Antennas Propag.*, vol. 59, no. 4, pp. 1269–1274, Apr. 2011.

[10] M. Müller, *Information Retrieval for Music and Motion*. Berlin, Germany: Springer, 2007.

[11] H. Sakoe and S. Chiba, "Dynamic programming algorithm optimization for spoken word recognition," *IEEE Trans. Acoust., Speech, Signal Process.*, vol. 26, no. 1, pp. 43–49, Feb. 1978.

[12] A. Corradini, "Dynamic time warping for off-line recognition of a small gesture vocabulary," in *Proc. IEEE ICCV Workshop Recognit., Anal., Tracking Faces Gestures Real-Time Syst.*, Vancouver, BC, Canada, Jul. 2011, pp. 82–89.

[13] G. E. Smith, K. Woodbridge, and C. J. Baker, "Radar micro-Doppler signature classification using dynamic time warping," *IEEE Trans. Aerosp. Electron. Syst.*, vol. 46, no. 3, pp. 1078–1096, Jul. 2010.

A Novel Marching-on-in-Degree Solver of Time Domain Parabolic Equation for Transient EM Scattering Analysis

Zi He and Ru Shan Chen

***Abstract*— A novel marching-on-in-degree (MOD) solver of 3-D time domain parabolic equation is proposed to solve the transient electromagnetic scattering from electrically large perfect electric conductor (PEC) targets. The finite difference (FD) scheme is applied to the spatial discretization, while the weighted Laguerre polynomials are used as the temporal basis functions. In this way, a large number of computational resources can be saved by using the FD scheme along the paraxial direction and the late-time stability can be guaranteed by the MOD method. Both the FD schemes of Crank–Nicolson and the alternating direction implicit types are discussed in this communication. Numerical results are given to demonstrate the accuracy and efficiency of the proposed method.**

***Index Terms*— Alternating direction implicit (ADI), Crank–Nicolson (CN), marching-on-in-degree (MOD) method, time domain parabolic equation (TDPE).**

I. INTRODUCTION

Nowadays, the transient electromagnetic (EM) scattering problem has been an important research topic in computational electromagnetics society. There are several popular numerical methods to analyze this kind of problems, such as the finite-different time-domain (FDTD) [1], the time domain integral equation [2]–[4], and the time domain finite element method [5]. However, a large number of computational resources are needed for these rigorous numerical methods. On the other hand, few computational resources are needed for the high frequency methods. However, the accuracy is very poor for complex structures. Therefore, more efficient method should be developed to study the transient EM scattering properties with encouraging accuracy.

The parabolic equation (PE) method [6]–[9] is an approximate form of the wave equation. By using the finite difference (FD) scheme to the paraxial direction, the calculation can be taken plane by plane along the paraxial direction. As a result, both the CPU time and memory requirement can be reduced significantly. The 2-D time-domain PE (2-D-TDPE) has been used to analyze the propagation for a long time [10]–[13]. Recently, we extended the 2-D-TDPE to 3-D case for the analysis of the transient EM scattering from electrically large target [14]. All of these works are based on FD schemes for both the spatial and temporal discretizations. There are two methods for the time-domain analysis, namely, the marching-on-in-time (MOT) and marching-on-in-degree (MOD) schemes. However, the MOT method may result in the late-time instability. The MOD scheme has been widely used in the FDTD [19], [20] and boundary integral method [21], [22] for transient analysis.

Manuscript received December 9, 2015; revised June 22, 2016; accepted July 30, 2016. Date of publication August 4, 2016; date of current version October 27, 2016. This work was supported in part by the National Natural Science Foundation of China under Grant 61431006 and Grant 61171041, in part by the Jiangsu Natural Science Foundation under Grant BK2012034, and in part by the Ph.D. Programs Foundation of Ministry of Education of China under Grant 20123219110018.

The authors are with the Department of Communication Engineering, Nanjing University of Science and Technology, Nanjing 210094, China (e-mail: 15850554055@163.com; eerschen@njust.edu.cn).

Color versions of one or more of the figures in this communication are available online at http://ieeexplore.ieee.org.

Digital Object Identifier 10.1109/TAP.2016.2598157